Research Paper
Computational Methods for Differential Equations
http://cmde.tabrizu.ac.ir
Vol. 14, No. 2, 2026, pp. 616-632
DOI:10.22034/cmde.2024.62350.2743

Mathematical modelling with optimal control of infectious diseases with vaccination

Henry M. Wanjala[1,*], **Mark O. Okongo**[1], **and Jimrise O. Ochwach**[2]
[1]Chuka University, Chuka, Kenya.
[2]Mama Ngina University College, Gatundu, Kenya.

Abstract

Mathematical models are critical in provision of information to the development of infections. Not with standing the effectiveness of vaccines, some vaccinated individuals nonetheless get infected. To deal with this, non- pharmaceutical measures inclusive of social distancing and handwashing are encouraged. This study offers a mathematical version that combines the effects of vaccination and social distancing, utilizing Kermack-McKendrick compartments and ordinary differential equations (ODE's). The study determines the basic reproduction number (R_0) by the use of the next generation matrix (NGM). If R_0 is less than 1, the ailment will in the end die out; if R_0 is more than 1, the ailment will continue to spread. Python simulations show that while vaccination and social distancing can reduce transmission, they may not be sufficient to eliminate the disease entirely. Isolation is critical for reducing transmission similarly, the efficacy of vaccines and the vaccination rate are crucial additives of a vaccination strategy. These techniques provide extra time for public health officers to put in force further measures, supplementing current processes. As we continue to come upon with new and evolving health challenges, the mixing of most reliable management strategies into epidemic modelling may be important. Further studies and interdisciplinary collaboration will enhance our capability to combat infectious sicknesses.

Keywords. Reproduction number, Stability analysis, Social distancing, Pontryagin's maximum principle.
2010 Mathematics Subject Classification. 39N25, 92R99.

1. Introduction

Respiratory ailments pose a massive hazard to our health and livelihoods, mainly in densely populated regions, wherein the infection can spread unexpectedly. COVID-19, due to the novel coronavirus, marks the third pandemic since 2002, after Severe Acute Respiratory Syndrome (SARS-CoV) in 2002 and Middle East Respiratory Syndrome Coronavirus (MERS-CoV) in 2012 [7]. Coronaviruses are highly contagious among individuals, causing profound effects in both populations and economies, and putting pressure on international healthcare structures [17].

The primary mode of transmission is through direct social contact with an infected person [3]. Furthermore, the virus can spread by touching contaminated surfaces or objects, as well as by inhaling droplets expelled by coughing, sneezing, or spitting, whether the person is symptomatic or not [19]. Extreme cases and fatalities occur mainly in older individuals and those with preexisting health conditions or weakened immune systems. The incubation period typically ranges from 2 to 14 days. Symptoms include fever, cough, fatigue, loss of taste or smell, sore throat, headaches, body aches, diarrhoea, skin rash, discoloration of extremities, red or irritated eyes, difficulty breathing, chest pain, and neurological symptoms. [24].

A study by [20] developed the SEIAR-SD model to forecast COVID-19 cases, the progression of the pandemic, and its duration in Rajasthan. The study emphasised that social distancing is a crucial factor in influencing the scale and duration of the pandemic. Vaccines play an important role in the preparation of the immune system of the body to protect against pathogens [16]. However, issues have arisen regarding reaching herd immunity due to the emergence of highly transmissible variants, reducing vaccine efficacy, and unequal vaccine distribution. Vaccination reduces the

Received: 04 July 2024; Accepted: 03 March 2025.
∗ Corresponding author. Email: teomat240@gmail.com .

chance of serious cases and loss of life, underscoring the importance of high vaccination coverage to protect healthcare systems from increased infections. Vaccination is a social responsibility, but issues related to hesitancy in vaccination and negative outcomes must be addressed [18].

Powerful intervention strategies for COVID-19 require an intensive understanding of transmission dynamics and prevention programs. Mathematical modelling has emerged as a precious tool for comprehending infectious disease dynamics, with recent studies indicating the cost-effectiveness of COVID-19 vaccination in low- and middle-income countries [31].

The optimisation of the disease control plan involves determining the maximum suitable management method(s), such as vaccination, quarantine, and the exceptional deployment approach for these strategies or their combination to minimise the effect of the infection. This minimisation turns complicated when resources are limited, and there are economic expenses associated with both the control measures and the sickness itself. Techniques that simulate the anticipated course of a virulent disease and together with the consequences of interventions, can quickly quantify the ability effect of a given approach [25]. A critical practical challenge, where mathematical modelling presents tremendous guide, is determining the distribution of constrained resources throughout an outbreak. Commonly, in preparation for a virulent disease, a set quantity of vaccines and other drugs are inventory-piled, in conjunction with the allocation of certain finances for other control measures like isolation and quarantine. As soon as a virulent disease starts off, the objective is to manage these resources optimally, given their limited availability [21].

Optimal control theory has proven to be a reliable tool in the knowledge of ways to reduce the spread of infectious illnesses by means of devising top-rated intervention techniques. This method involves minimising both the rate of transmission and the cost of enforcing control measures, or both [22]. Often, there's no earlier knowledge of the number of susceptible, infected, and recovered individuals necessary to formulate and solve the optimal control problem. In a scenario where prior knowledge is absent, a strategy based on an analytic function was proposed by [22], eliminating the need for prior scenario knowledge. A study by [9] focused on time-dependent controls using optimal control theory. This strategy sought to minimise both disease burden and intervention costs. They derived and numerically solved the optimality system, offering a thorough analysis of the potential outcomes of the model. Their strategy aimed toward minimising each of the disease burden and the intervention costs. They derived the optimality equation and solved it numerically, offering a comprehensive evaluation of the feasible results of the model.

In the absence of effective therapeutics, countries have depended on vaccines and non-pharmaceutical interventions (NPIs) to diminish the epidemic's effect. With the supply of COVID-19 vaccines, it's far vital to assess their effect, specifically in light of imperfect vaccines, and refine present mathematical models to contain these issues.

2. Model formulation and development

The model divides the total population, denoted by N, into seven distinct groups: Susceptible (S), Vaccinated (V), Exposed (E), Symptomatic (I), Asymptomatic (A), Isolated (J), and Recovered (R). The population grows due to the births of susceptible individuals at a rate Λ and decrease as susceptibles are exposed to infection at a rate λ. Social distancing, characterized by an SD parameter ranging from approximately 0 (no social distancing) to 1 (effective social distancing), is practiced within the population. Vaccination occurs at a rate α, but since the vaccine is not fully effective, a fraction (1 - θ) of vaccinated individuals can still become infected. The efficacy of the vaccine, θ, ranges from 0 (no protection) to 1 (full protection). After an incubation period of duration ω, a fraction ν of the exposed become asymptomatic, while the remainder (1 - η) become symptomatic. Asymptomatic individuals recover naturally at a rate ρ_A, while symptomatic ones are isolated at a rate γ. Isolated individuals recover at a rate ρ_J. Additionally, there's a constant natural mortality rate of μ. The flow chart of the model is shown in Figure 1.

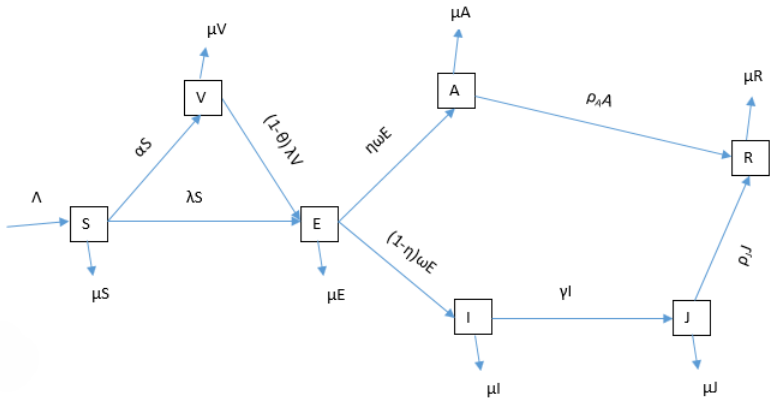

FIGURE 1. Model flow chart.

The model equations are represented in Eq. (2.1)

$$\begin{cases} \dfrac{dS}{dt} = \Lambda - (\alpha + \lambda + \mu)S, \\ \dfrac{dV}{dt} = \alpha S - (\mu + (1-\theta)\lambda)V, \\ \dfrac{dE}{dt} = \lambda S + ((1-\theta)\lambda)V - (\mu + \omega)E, \\ \dfrac{dA}{dt} = \eta\omega E - (\mu + \rho_A)A, \\ \dfrac{dI}{dt} = (1-\eta)\omega E - (\mu + \gamma)I, \\ \dfrac{dJ}{dt} = \gamma I - (\mu + \rho_J)J, \\ \dfrac{dR}{dt} = \rho_A A + \rho_J J - \mu R. \end{cases} \tag{2.1}$$

The force of infection, λ is given by Eq. (2.2):

$$\lambda = \beta(1 - SD)(A + \epsilon I)/N. \tag{2.2}$$

The model parameters and the parameter values are shown in Table 1.

3. Model analysis

3.1. **Positivity of the solution.** The model system Eq. (2.1) deals with living organisms and thus the associated state variables are non-negative for all the time $t > 0$. Thus, the solutions to model Eq. (2.1) with initial data is positive for all time $t > 0$.

Theorem 3.1. *The region* $\mathcal{D} = \{(S(t), V(t), E(t), A(t), I(t), J(t), R(t)) \in \mathfrak{R}^7_+ : N(t) \leq \frac{\Lambda}{\mu}\}$ *is positively invariant and attracting with respect to model Eq.* (2.1).

TABLE 1. Parameter values.

Symbol	Parameter	Value	Source
Λ	Recruitment rate by birth	0.46439 days^{-1}	[1]
μ	Natural death rate	0.11 days^{-1}	[36]
α	Rate of vaccination	0.0043	[2]
θ	Vaccine efficacy rate	0.8	[13]
ω	Latency period	0.13	[36]
η	Fraction of those Asymptomatic but Infectious	0.7	[36]
γ	Rate of hospitalisation	0.0833	[26]
γ	Rate of hospitalisation	0.0833	[4]
ρ_A	Recovery rate of asymptomatic	0.13978	[4]
ρ_J	Recovery rate of hospitalised	0.0701	[12]
β	Effective contact rate	0.5	[35]
ϵ	Infectivity factor	0.48	[39]

Proof. Solving the first equation of Eq. (2.1) for S(t) at time, $t > 0$, it is obtained that:

$$\begin{cases} \frac{dS}{dt} = \Lambda - (\alpha + \lambda + \mu)S, \\ \frac{dS}{dt} \geq -(\alpha + \lambda + \mu)S, \\ \int \frac{dS}{S} \geq -\int (\alpha + \lambda + \mu)dt, \\ \int_{S(0)}^{S} \frac{dS}{S} \geq -\int (\alpha + \lambda + \mu)dt, \\ LnS - LnS(0) \geq -\int (\alpha + \lambda + \mu)dt, \\ Ln\frac{S}{S(0)} \geq -\int (\alpha + \lambda + \mu)dt, \\ \frac{S}{S(0)} \geq e^{-\int(\alpha+\lambda+\mu)dt}, \\ S \geq S(0)e^{-\int(\alpha+\lambda+\mu)dt}. \end{cases} \tag{3.1}$$

Clearly, S(0) $e^{-\int(\alpha+\lambda+\mu)dt}$ is a non- negative function of t, thus S(t) stays positive.

Equivalent demonstrations can be constructed to affirm the positivity of various variables by employing the relevant equations within the system. This implies that the solutions to system 1, given non-negative initial conditions such that $V(t) > 0, E(t) > 0, A(t) > 0, I(t) > 0, J(t) > 0$, and $R(t) > 0$, will persist in non-negativity for all time instances $t \geq 0$. □

3.2. **Invariant region.**

Theorem 3.2. *For the initial conditions* $S(0) = S_0 > 0, V(0) = V_0 > 0, E(0) = E_0 > 0, A(0) = A_0 > 0, I(0) = I_0 > 0, J(0) = J_0 > 0, R(0) = R_0 > 0$, *the solution of system* (2.1) *are contained in the region* $\mathcal{H} \in \mathfrak{R}_+^7$, *defined by*

$$\mathcal{H} = [S(t), V(t), E(t), A(t), I(t), J(t), R(t)] \in \mathfrak{R}_+^7 : N(t) \leq \frac{\Lambda}{\mu}\}. \tag{3.2}$$

Theorem 3.3. *For the initial conditions* $S(0) = S_0 > 0, V(0) = V_0 > 0, E(0) = E_0 > 0, A(0) = A_0 > 0, I(0) = I_0 > 0, J(0) = J_0 > 0, R(0) = R_0 > 0$, *the solution of system Eq.* (2.1) *are contained in the region* $\mathcal{H} \in \mathfrak{R}_+^7$, *defined by*

$$\mathcal{H} = [S(t), V(t), E(t), A(t), I(t), J(t), R(t)] \in \mathfrak{R}_+^7 : N(t) \leq \frac{\Lambda}{\mu}\}. \tag{3.3}$$

Proof. Summation of all equations of model system Eq. (2.1) gives:

$$\frac{dN(t)}{dt} = \frac{dS(t)}{dt} + \frac{dV(t)}{dt} + \frac{dE(t)}{dt} + \frac{dA(t)}{dt} + \frac{dI(t)}{dt} + \frac{dJ(t)}{dt} + \frac{dR(t)}{dt}. \tag{3.4}$$

The change in the total population is defined by,

$$\frac{dN}{dt} = \Lambda - \mu N, \tag{3.5}$$

which gives

$$\frac{dN}{dt} \leq \Lambda - \mu N. \tag{3.6}$$

Integrating Equation (4.1) by using the method of separation of variables and taking $N(0) = N_0$, the solution of the Equation (4.1) above is given by:

$$N(t) \leq \frac{\Lambda}{\mu} - \left(\frac{\Lambda}{\mu} - N_0\right) e^{-\mu t}, \quad \text{where } N_0 = N(0). \tag{3.7}$$

The study of [5], developed the Birkhoff-Rota theorem, which we note that if, $N_0 < \frac{\Lambda}{\mu}$, then N $\to \frac{\Lambda}{\mu}$ asymptotically as t $\to \infty$ in Equation (3.1) and the total population size, N $\to \frac{\Lambda}{\mu}$, which means that, $0 \leq N \leq \frac{\Lambda}{\mu}$. Therefore, all the feasible solutions in the model converge in the region $\mathcal{H}$. □

4. Analysis of disease free equilibrium state (DFE), E_0 and basic reproduction number

4.1. **Disease free equilibrium, E_0.** The Disease Free Equilibrium (E_0), is assumed to be the point where there's no infection in the community. The model system Eq. (2.2) compartments are set to 0, such that, S = 0, V = 0, E = 0, A = 0, I = 0, J = 0, R = 0. Simplifying, the DFE point for the system is defined as follows:

$$E_0 = \left(\frac{\beta(1-SD)\Lambda}{\alpha+\mu}, \frac{\beta(1-SD)\alpha\Lambda}{\mu(\alpha+\mu)}, 0, 0, 0, 0, 0\right) \tag{4.1}$$

4.2. **Basic reproduction number ($\mathbf{R}_0$).** The study of [14, 15] established the concept of the basic reproduction number, which quantifies the average number of secondary infections caused by a primary infected individual over the course of their entire period of infectiousness. To calculate this number, we employed the next generation matrix approach outlined by [34] and illustrated by [35] utilizing matrices F and V to represent new infections and transitions, respectively. The two matrices are as shown below:

$$\mathcal{F} = \begin{bmatrix} 0 & m\beta_0 + (1-\theta)\eta & m\beta_0\epsilon + (1-\theta)\eta\epsilon & 0 \\ 0 & 0 & 0 & 0 \\ 0 & 0 & 0 & 0 \\ 0 & 0 & 0 & 0 \end{bmatrix}, \tag{4.2}$$

and

$$\mathcal{V} = \begin{bmatrix} -k_1 & 0 & 0 & 0 \\ \eta\omega & -k_2 & 0 & 0 \\ (1-\eta)\omega & 0 & -k_3 & 0 \\ 0 & 0 & \gamma & -k_4 \end{bmatrix}. \tag{4.3}$$

The reproduction number is the spectral radius of FV^{-1}. Thus, the effective reproduction number for the epidemiological system is:

$$\mathcal{R}_v = \frac{\eta\omega(\eta(1-\theta) + m\beta_0)}{k_1 k_2} + \frac{(1-\eta)\omega(\epsilon\eta(1-\theta) + \epsilon m\beta_0)}{k_1 k_3}, \tag{4.4}$$

$\mathcal{R}_v$ is the control reproduction number of an epidemic. It measures the estimated number of new infections generated by an index case in a community with a vaccination program set up.

Similarly, the basic reproduction number $\mathcal{R}_0$ is established by setting the parameter $\theta = 0$ in equation above Eq.(4.4), resulting to:

$$\mathcal{R}_0 = \frac{\eta\omega(\eta + m\beta_0)}{k_1 k_2} + \frac{(1-\eta)\omega(\epsilon\eta + \epsilon m\beta_0)}{k_1 k_3}. \tag{4.5}$$

4.3. **Stability analysis of the disease-free equilibrium (DFE) point.**

4.3.1. ***Local stability analysis of the disease-free equilibrium point.*** A study was done by [10] who introduced a theorem aimed at performing local stability assessment of an ordinary differential equation system through the application of numerical techniques.

Theorem 4.1. *Assume the first order partial derivatives of f and g are continuous in some open set containing the equilibrium point (x̂,ŷ). Then, the equilibrium is locally asymptotically stable if*

(1) *Tr($\mathcal{J}_f$) < 0,*

(2) *Det ($\mathcal{J}_f$) > 0,*

where, J is the Jacobian matrix evaluated at the equilibrium. In addition, the equilibrium is unstable if either Tr(J) > 0 or Det(J) < 0.

Computing the Jacobian matrix of Eq.(2.1) at DFE, it yields Eq.(4.6):

$$\mathcal{J}_f = \begin{bmatrix} -k_1 & 0 & 0 & -A_1 & -I_1 & 0 & 0 \\ \alpha & -\mu & 0 & -A_2 & -I_2 & 0 & 0 \\ 0 & 0 & -k_3 & A_3 & I_3 & 0 & 0 \\ 0 & 0 & \eta\omega & -k_4 & 0 & 0 & 0 \\ 0 & 0 & (1-\eta)\omega) & 0 & -k_5 & 0 & 0 \\ 0 & 0 & 0 & 0 & \gamma & -k_6 & 0 \\ 0 & 0 & 0 & \rho_A & 0 & \rho_J & -\mu \end{bmatrix}, \tag{4.6}$$

where:

$$k_1 = \mu + \alpha, \quad k_3 = \mu + \omega, \quad k_4 = -\mu + \rho_A, k_5 = \mu + \gamma,$$
$$k_6 = \mu + \rho_J, \quad m = \frac{\beta(1-SD)\Lambda}{\alpha+\mu}, \quad n = \frac{\beta(1-SD)\alpha\Lambda}{\mu(\alpha+\mu)},$$
$$A_1 = m, \quad A_2 = (1-\theta), \quad A_3 = A_1 + A_2,$$
$$I_1 = \epsilon m, \quad I_2 = (1-\theta)\epsilon n, \quad I_3 = I_1 + I_2.$$

Based on the matrix provided in Eq.(4.6) and the numerical analysis of the parameters outlined in Table 1, it is clear that:

(1) Tr($\mathcal{J}_f$) < 0 , and
(2) Det ($\mathcal{J}_f$) > 0.

Thus, the DFE is locally asymptotically stable. This suggests that, without significant alterations or external influences, the disease should stay at minimal levels or be well managed within the population. Nonetheless, it's crucial to understand that local stability doesn't ensure sustained control of the disease in the long run, particularly if circumstances evolve or new variables emerge. Hence, ongoing vigilance and adjustment of strategies are essential for effectively managing the epidemic.

4.3.2. ***Local stability analysis of the endemic equilibrium point.*** Assume the first order partial derivatives of f and g are continuous in some open set containing the equilibrium point (x̂,ŷ). Then, the equilibrium is locally asymptotically stable if,

(1) Tr($\mathcal{J}_f$) < 0 , and
(2) Det ($\mathcal{J}_f$) > 0

where, J is the Jacobian matrix evaluated at the equilibrium. In addition, the equilibrium is unstable if either Tr(J) > 0 or Det(J) < 0.

Computing the Jacobian matrix of Eq. (2.1) at DFE, it yields Eq. (4.7):

$$\mathcal{J}_f = \begin{bmatrix} -(k_1+\lambda) & 0 & 0 & -A_1 & -I_1 & 0 & 0 \\ \alpha & -\mu-(1-\theta)\lambda & 0 & -A_2 & -I_2 & 0 & 0 \\ \lambda & (1-\theta)\lambda & -k_3 & A_3 & I_3 & 0 & 0 \\ 0 & 0 & \eta\omega & -k_4 & 0 & 0 & 0 \\ 0 & 0 & (1-\eta)\omega) & 0 & -k_5 & 0 & 0 \\ 0 & 0 & 0 & 0 & \gamma & -k_6 & 0 \\ 0 & 0 & 0 & \rho_A & 0 & \rho_J & -\mu \end{bmatrix}, \tag{4.7}$$

where

$$k_1 = \mu+\alpha, \quad k_3 = \mu+\omega, \quad k_4 = -\mu+\rho_A, \quad k_5 = \mu+\gamma,$$
$$k_6 = \mu+\rho_J, \quad m = \frac{\beta(1-SD)\Lambda}{\alpha+\mu}, \quad n = \frac{\beta(1-SD)\alpha\Lambda}{\mu(\alpha+\mu)},$$
$$A_1 = m, \quad A_2 = (1-\theta), \quad A_3 = A_1+A_2,$$
$$I_1 = \epsilon m, \quad I_2 = (1-\theta)\epsilon n, \quad I_3 = I_1+I_2.$$

Based on the matrix provided in Eq. (4.7) and the numerical analysis of the parameters outlined in Table 1, it is concluded that:

(1) $\mathrm{Tr}(\mathcal{J}_f) < 0$, and
(2) Det $(\mathcal{J}_f) > 0$.

Thus, the EE is locally asymptotically stable.

4.3.3. ***Global stability analysis of the disease-free equilibrium point***. We employ the Lyapunov-Krasovskii method for analysing the global asymptotic stability.

Theorem 4.2. *Consider the autonomous system defined by $\dot{x} = f(x)$, with the equilibrium point of interest being the origin. Let $A(x)$ denote the Jacobian matrix of the system, $A(x) = \frac{\partial f}{\partial x}$. If the matrix $F = A + A^T$ is a negative neighbourhood Ω, then, the equilibrium point at the origin is asymptotically stable. A Lyapunov function for this system is*

$$V(x) = f^T(x)f(x). \tag{4.8}$$

If Ω is the entire state space and, in addition, $V(x) \to \infty$, $[||x||] \to \infty$, then, the equilibrium point is said to be globally asymptotically stable as expounded in [39].

Global stability analysis entails creating the Jacobian matrix of the model system in Eq. (2.1) and solving it at the Disease-Free Equilibrium (DFE), as depicted in the matrix in Eq. (4.9)

$$F(x) = \begin{bmatrix} -k_1 & 0 & 0 & -A_1 & -I_1 & 0 & 0 \\ \alpha & -\mu & 0 & -A_2 & -I_2 & 0 & 0 \\ 0 & 0 & -k_3 & A_3 & I_3 & 0 & 0 \\ 0 & 0 & \eta\omega & -k_4 & 0 & 0 & 0 \\ 0 & 0 & (1-\eta)\omega) & 0 & -k_5 & 0 & 0 \\ 0 & 0 & 0 & 0 & \gamma & -k_6 & 0 \\ 0 & 0 & 0 & \rho_A & 0 & \rho_J & -\mu \end{bmatrix}, \tag{4.9}$$

where

$$k_1 = \mu+\alpha, \quad k_3 = \mu+\omega, \quad k_4 = -\mu+\rho_A, \quad k_5 = \mu+\gamma,$$
$$k_6 = \mu+\rho_J, \quad m = \frac{\beta(1-SD)\Lambda}{\alpha+\mu}, \quad n = \frac{\beta(1-SD)\alpha\Lambda}{\mu(\alpha+\mu)},$$

$$A_1 = m, \qquad A_2 = (1-\theta), \qquad A_3 = A_1 + A_2,$$
$$I_1 = \epsilon m, \qquad I_2 = (1-\theta)\epsilon n, \qquad I_3 = I_1 + I_2.$$

From the matrix Eq. (4.9) above, $\hat{F}(x)$ is as shown in matrix Eq. (4.11):

$$\hat{F}(x) = F^T(x) + F(x) \tag{4.10}$$

This implies that $\hat{F}(x)$ is as in matrix (4.11):

$$\hat{F}(x) = \begin{bmatrix} 2k_1 & \alpha & 0 & -A_1 & -I_1 & 0 & 0 \\ \alpha & -2\mu & 0 & -A_2 & -I_2 & 0 & 0 \\ 0 & 0 & -2k_3 & A_3+\eta\omega & I_3+(1-\eta)\omega & 0 & 0 \\ -A_1 & -A_2 & \eta\omega + A_3 & -2k_4 & 0 & 0 & \rho_A \\ -I_1 & -I_2 & (1-\eta)\omega + I_3 & 0 & -2k_5 & \gamma & 0 \\ 0 & 0 & 0 & 0 & \gamma & -2k_6 & \rho_J \\ 0 & 0 & 0 & \rho_A & 0 & \rho_J & -2\mu \end{bmatrix}, \tag{4.11}$$

where:

$$k_1 = \mu + \alpha, \qquad k_3 = \mu + \omega, \qquad k_4 = -\mu + \rho_A, \qquad k_5 = \mu + \gamma,$$
$$k_6 = \mu + \rho_J, \qquad m = \frac{\beta(1-SD)\Lambda}{\alpha+\mu}, \qquad n = \frac{\beta(1-SD)\alpha\Lambda}{\mu(\alpha+\mu)},$$
$$A_1 = m, \qquad A_2 = (1-\theta), \qquad A_3 = A_1 + A_2,$$
$$I_1 = \epsilon m, \qquad I_2 = (1-\theta)\epsilon n, \qquad I_3 = I_1 + I_2.$$

If A is a negative definite matrix of order n that is, all eigenvalues are negative, then $\mathrm{Tr}(\hat{F}(x)) < 0$. If n is even, $\mathrm{Det}(\hat{F}(x)) > 0$, and if n is odd, $\mathrm{Det}(\hat{F}(x)) < 0$. Since $\mathrm{Tr}(\hat{F}(x)) < 0$ and $\mathrm{Det}(\hat{F}(x)) > 0$, then, the equilibrium point is said to be asymptotically unstable.

It suggests the potential for the disease to exhibit unpredictable or chaotic behavior, leading to recurrent outbreaks or sustained transmission within the population. This instability indicates that the disease may not be easily controlled or eradicated through conventional measures of vaccination and social distancing only, and efforts to manage the epidemic may face significant challenges. It underscores the importance of continuous monitoring, adaptation of control strategies, and possibly the development of novel interventions to mitigate the spread of the disease and minimize its impact on public health.

5. Numerical simulations

To examine the impacts of different interventions in preventing and managing COVID-19, we performed numerical simulations using the system model Eq. (2.1). The model incorporated parameter values from existing research, with some estimates to ensure meaningful analysis for this study.

We conducted simulations using the parameter values listed in Table 1, spanning the time period of $0 \leq t \leq 300$ days, reflecting the expected duration of the disease progression. Python software, with Jupyter as the integrated development environment (IDE), was utilized for these simulations. The results are visually represented through graphical illustrations.

5.1. **Numerical simulation on the impact of interventions.** Figure 2 depicts the scenario where disease transmission occurs without any intervention. The graph illustrates that symptomatic patients continue to exist within the community, leading to the disease becoming endemic. In contrast, Figure 3 shows the effects of interventions such as vaccination, isolation, and social distancing, applied simultaneously. These interventions result in a decrease in infections and a delay in the peak day, allowing for the enhancement of health facilities. However, there is an increase in susceptible individuals in the population, indicating that the disease could still become endemic despite these measures. Therefore, it is imperative for public health officials to implement additional intervention strategies.

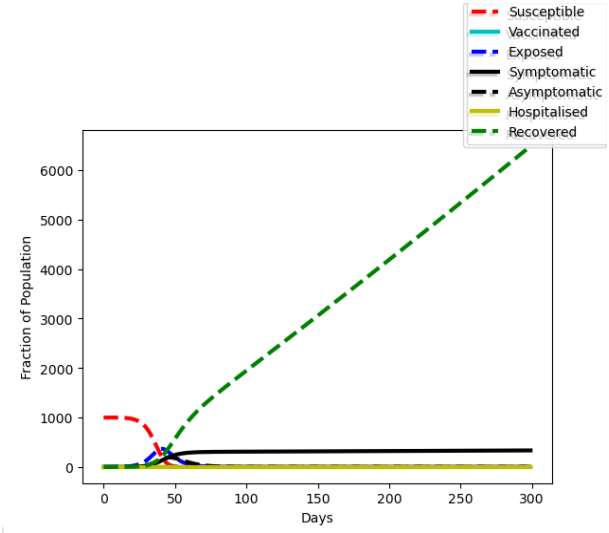

FIGURE 2. Absence of interventions.

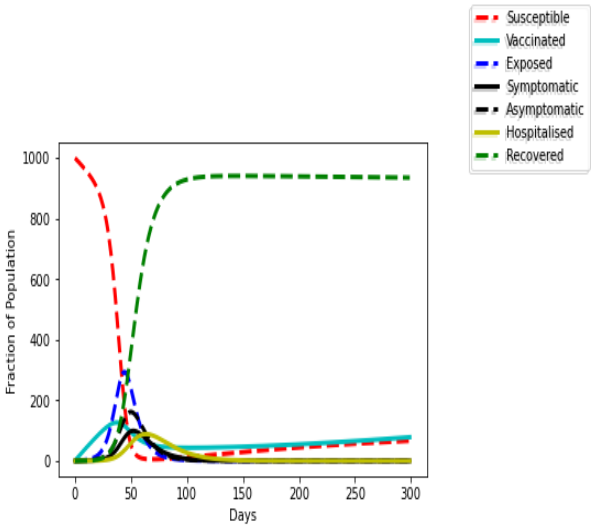

FIGURE 3. Presence of interventions.

5.2. **Numerical simulation on the impact of social distancing.** Figures 4 and 5 demonstrate the importance of Social Distancing as a Non-Pharmaceutical Intervention (NPI) in reducing transmission. Both graphs show that increasing compliance rates result in decreased infected cases and a delay in the expected peak day.

The figures indicate that the effect of social distancing is more significant on asymptomatic individuals who do not take precautionary measures compared to symptomatic individuals.

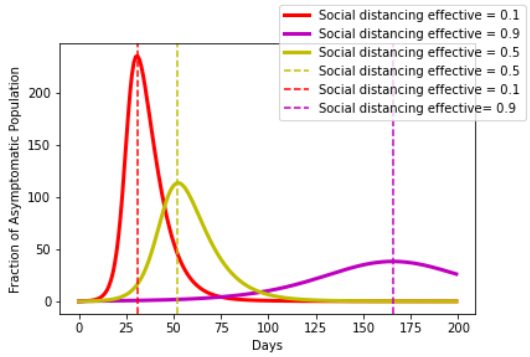

FIGURE 4. Impact of social distancing on asymptomatics.

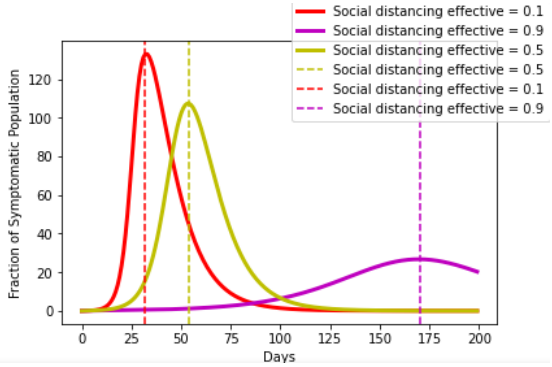

FIGURE 5. Impact of social distancing on symptomatics.

5.3. **Numerical simulation on the impact of vaccine efficacy level.** Figure 6 demonstrates how the vaccine efficacy rate affects the number of asymptomatic cases. When the efficacy rate exceeds 90%, the cases decrease to zero. Similarly, Figure 7 shows the impact of vaccine efficacy on symptomatic cases.

However, achieving a vaccine efficacy of over 90% may be unrealistic. Therefore, it is essential to combine the vaccine efficacy with vaccination rate and implement additional interventions to effectively manage the situation.

5.4. **Numerical simulation on the impact of vaccination rate and efficacy.** Increasing both the efficacy of the vaccine and the proportion of the population vaccinated leads to a reduction in the transmission rate. The

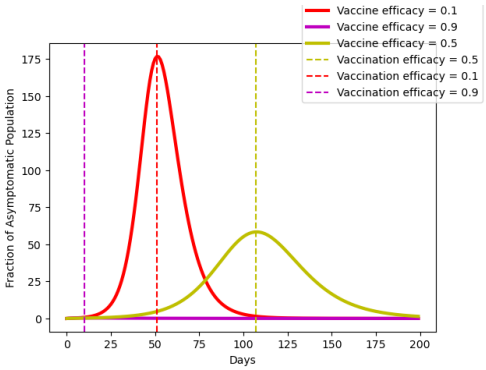

FIGURE 6. Impact of vaccine efficacy level on asymptomatics.

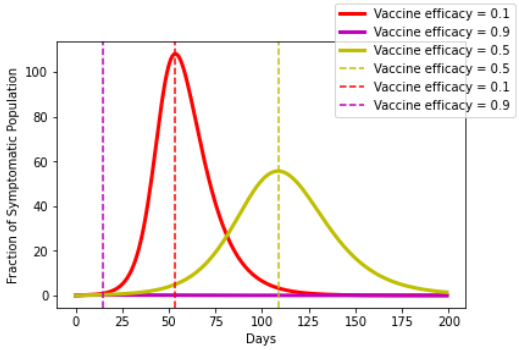

FIGURE 7. Impact of vaccine efficacy level on symptomatics.

vaccination rate and vaccine efficacy rate interact multiplicatively, underscoring the importance of considering both factors together. This interaction is illustrated in the Figure 8 below.

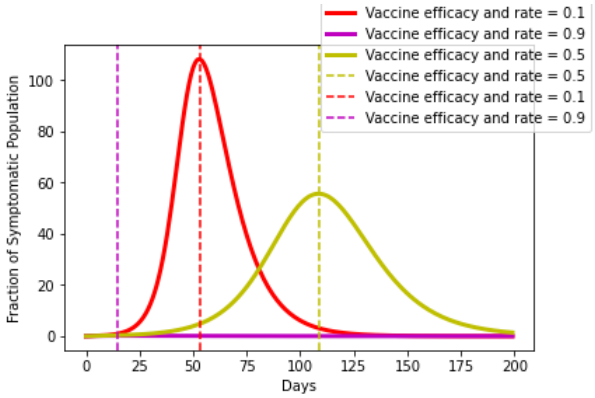

FIGURE 8. Effect of vaccine efficacy and rate.

6. Extension of the model into optimal control

In this section, we delve into the optimal control of model Eq. (2.1), which describes the interaction between media awareness and susceptible individuals, as well as the vaccination efforts within the susceptible population. The main goal of optimal control here is to decrease the total number of infected individuals while minimizing the related costs. We apply optimal control to system Eq. (2.1) to analyze the impacts of continuous media awareness and vaccination strategies in mitigating the COVID-19 outbreak. To this end, we introduce a set of time-dependent control variables, $u_1(t)$ and $u_2(t)$, where:

(i) $u_1(t)$ represents efforts directed towards raising awareness among susceptible individuals through various media outlets.
(ii) $u_2(t)$ represents efforts aimed at promoting the continuous vaccination of susceptible individuals.

For simplicity, we denote $u_1(t)$ as u_1 and $u_2(t)$ as u_2. By integrating these intervention strategies into the model Eq. (2.1), we derive an optimal control model represented by Eq. (6.1):

$$\begin{cases} \dfrac{dS}{dt} = \Lambda - (\alpha + \lambda + \mu + u_1 + u_2)S, \\ \dfrac{dV}{dt} = \alpha S + u_2 S - (\mu + (1-\theta)\lambda)V, \\ \dfrac{dE}{dt} = \lambda S + ((1-\theta)\lambda)V - (\mu + \omega)E, \\ \dfrac{dA}{dt} = \eta\omega E - (\mu + \rho_A)A, \\ \dfrac{dI}{dt} = (1-\eta)\omega E - (\mu + \gamma)I, \\ \dfrac{dJ}{dt} = \gamma I - (\mu + \rho_J)J, \\ \dfrac{dR}{dt} = \rho_A A + \rho_J J + u_1 S - \mu R. \end{cases} \tag{6.1}$$

The optimal control variables u_1 and u_2 minimise the objective function while adhering to the constraints of the system Eq. (6.1). The objective function is specified as follows:

$$J(u_1, u_2) = \min_{u_1, u_2} \int_0^{t_f} \left[A_1 S(\tau) + A_2 V(\tau) + B_1 u_1^2(\tau) + B_2 u_2^2(\tau)\right] d\tau, \tag{6.2}$$

where t_f is the predetermined final time, and the positive coefficients A_1, A_2, B_1, and B_2 are constants that balance the cost and the number of infected individuals at time t. In this study, we use the quadratic form for measuring control costs, as commonly used in [30] and [6], due to its non-linear nature. The primary goal is to determine the optimal control (u_1^*, u_2^*) such that:

$$J(u_1^*, u_2^*) = \min\left(J(u_1, u_2) : u_1, u_2 \in U\right).$$

The controls u_1 and u_2 are assumed to be at least Lebesgue measurable on $[0, t_f]$ as described by the work of [23].

6.1. **Existence of Optimal Control Problem.**

Theorem 6.1. *The model Eq. (6.1) admits $u^* \in U_{ad}$ that verifies*

$$J(u^*) = \min_{u \in U_{ad}} J(u).$$

Proof. To show the existence of an optimal control, we have to check the following assertions.

- Non-empty Solution Set: By the theory of differential equations, for a continuous, bounded system like Eq.(6.1), the solution set is non-empty when an initial condition and measurable control functions $u_1(t)$ and $u_2(t)$ are given over a finite time interval $[0, t_f]$.
- Closed and Convex Control Set U_{ad}: U_{ad} is defined as the admissible set of control functions where each control is Lebesgue measurable and bounded. Convexity holds because any convex combination of admissible controls is also in U_{ad}, and the set is closed under pointwise limits.
- Bounded Right-Hand Side: For system Eq.(6.1), each right-hand side expression is bounded by a linear function of the controls u_1, u_2 and the state variables, since the controls only appear linearly in each equation. Thus, these expressions satisfy the required bound.
- Convex Lagrangian $L(S, V, u_1, u_2)$: The objective function $J(u_1, u_2)$ is quadratic in u_1 and u_2, so the Lagrangian L associated with it remains convex in U_{ad}, as a sum of convex functions (such as the quadratic forms u_1^2 and u_2^2) is also convex.
- Coercivity Condition: For the Lagrangian $L(S, V, u_1, u_2)$ to satisfy coercivity, there exist constants $\alpha_1 > 0$, $\alpha_2 > 0$, and $\rho > 1$ such that:

  $$L(S, V, u_1, u_2) \geq \alpha_1 + \alpha_2(|v|^2 + |u|^2 + |w|^2)^{\rho/2}.$$

by selecting α_1 and α_2 so that the terms dominate as $|u| \to \infty$, enforcing a lower bound on L, thereby satisfying the coercivity requirement for an optimal solution.

Together, these conditions confirm the existence of an optimal control u^* in U_{ad} that minimizes $J(u)$.

□

6.2. **Characterisation of the optimal control.** Now, to solve the optimal control problem Eq. (6.1), we have formulated the Lagrangian equation as follows:

$$L(t,x,u) = \frac{dJ}{dt} = A_1 S(t) + A_2 V(t) + B_1 u_1^2(t) + B_2 u_2^2(t).$$

The necessary conditions that an optimal control must satisfy are derived from Pontryagin's Maximum Principle [11, 32].

To minimize the Lagrangian, we have formulated the Hamiltonian equation by:

$$H(t,x,u,\xi) = \frac{dJ}{dt} + \sum_{i=1}^{7} P_i f_i = L(t,x,u) + \sum_{i=1}^{7} P_i f_i,$$

where $L(t,x,u) = A_1 S + A_2 V + B_1 u_1^2(t) + B_2 u_2^2(t)$ and f_i, $i = 1,2,3,4,5,6,7$ are the right-hand side components of (6.1). The variables $P = (P_1, P_2, P_3, P_4, P_5, P_6, P_7) \in \mathbb{R}^7$ are costate variables associated with the state variables S, V, E, A, I, J and R, which can be determined from the second partial derivatives of H with respect to the state variables as follows:

$$\begin{aligned} H &= L(t,x,u) + P_1(\Lambda - (\alpha + \lambda + \mu + u_1 + u_2)S) \\ &\quad + P_2(\alpha S + u_2 S - (\mu + (1-\theta)\lambda)V) \\ &\quad + P_3(\lambda S + ((1-\theta)\lambda)V - (\mu + \omega)E) \\ &\quad + P_4(\eta\omega E - (\mu + \rho_A)A) \\ &\quad + P_5((1-\eta)\omega E - (\mu + \gamma)I) \\ &\quad + P_6(\gamma I - (\mu + \rho_J)J) \\ &\quad + P_7(\rho_A A + \rho_J J + u_1 S - \mu R), \end{aligned} \tag{6.3}$$

where

$$\frac{dP_1}{dt} = -\frac{\partial H}{\partial S}, \quad \frac{dP_2}{dt} = -\frac{\partial H}{\partial V}, \quad \frac{dP_3}{dt} = -\frac{\partial H}{\partial E}, \quad \frac{dP_4}{dt} = -\frac{\partial H}{\partial A}, \quad \frac{dP_5}{dt} = -\frac{\partial H}{\partial I}, \quad \frac{dP_6}{dt} = -\frac{\partial H}{\partial J}, \quad \frac{dP_7}{dt} = -\frac{\partial H}{\partial R}.$$

Thus,

$$\begin{aligned} \dot{P}_1 &= (\alpha + \lambda + \mu + u_1 + u_2)P_1 - P_2 u_2 - P_3 \alpha - P_7 u_1, \\ \dot{P}_2 &= (\mu + (1-\theta)\lambda)P_2 - (1-\theta)\lambda P_3, \\ \dot{P}_3 &= (\mu + \omega)P_3 - \eta\omega P_4 - (1-\eta)\omega P_5, \\ \dot{P}_4 &= (\mu + \rho_A)P_4 - \rho_A P_7, \\ \dot{P}_5 &= (\mu + \gamma)P_5 - \gamma P_6, \\ \dot{P}_6 &= (\mu + \rho_J)P_6 - \rho_J P_7, \\ \dot{P}_7 &= \mu P_7, \end{aligned} \tag{6.4}$$

with transversality conditions:

$$\begin{aligned} &P_1(t_f) = P_2(t_f) = P_3(t_f) = P_4(t_f), \\ &P_5(t_f) = P_6(t_f) = P_7(t_f), \\ &L(t,x,u) = \frac{1}{2}(B_1 u^2{}_1 + B_2 u^2{}_2). \end{aligned} \tag{6.5}$$

6.3. **Optimal Control.** The optimal controls $u^*{}_1$ and $u^*{}_2$ are found by solving,

$$\frac{\partial H}{\partial u_1} = 0,$$
$$\frac{\partial H}{\partial u_2} = 0.$$

Computing the partial derivatives of H with respect to u_1 and u_2

$$\frac{\partial H}{\partial u_1} = B_1 u_1 - P_1 S + P_7 S,$$

setting,

$$\frac{\partial H}{\partial u_1} = 0,$$
$$B_1 u_1 - P_1 S + P_7 S = 0,$$
$$u_1 = (P_1 S - P_7 S)\frac{1}{B_1},$$

similarly for u_2,

$$\frac{\partial H}{\partial u_2} = B_2 u_2 - P_1 S + P_2 S,$$

setting,

$$\frac{\partial H}{\partial u_1} = 0,$$
$$B_2 u_2 - P_1 S + P_2 S = 0,$$
$$u_2 = (P_1 S - P_2 S)\frac{1}{B_2}.$$

Since, the controls u_1 and u_2 are bounded between 0 and 1, we use the projection operator,

$$u_1(t) = \min\{1, \max\{0, u_\Delta\}\}, \quad u_2(t) = \min\{1, \max\{0, u_\nabla\}\},$$

where

$$u_\Delta = \frac{P_1 S - P_7 S}{B_1}, \qquad u_\nabla = \frac{P_1 S - P_2 S}{B_2}.$$

The optimal control set $\{u_1^*(t), u_2^*(t)\}$ is given by:

$$u_1(t) = \min\left\{1, \max\left\{0, \frac{P_1 S - P_7 S}{B_1}\right\}\right\}, \qquad u_2(t) = \min\left\{1, \max\left\{0, \frac{P_1 S - P_2 S}{B_2}\right\}\right\}.$$

6.4. **Numerical Simulation of the Optimal Control Set.** The epidemiological model presented here describes the dynamics of a population with respect to different compartments representing various stages of disease progression and intervention measures. Each curve in the plots represents the evolution over time of a specific compartment in the population. Here are the real-life meanings of each curve:

- **S (Susceptible); Figure 9**:
  No Controls: This curve shows the number of individuals in the population who are susceptible to infection over time without any intervention. Typically, this number decreases as people get infected.
  With Controls: This curve shows the number of susceptible individuals when control measures are applied (e.g., vaccination or social distancing). Controls are expected to reduce the rate of infection, slowing down the decline in the susceptible population.

- **V (Vaccinated); Figure 10**:
  No Controls: If no vaccination is applied, the number of vaccinated individuals will remain zero or very low.
  With Controls: This curve shows the number of individuals who have been vaccinated over time. With vaccination as a control measure, this number should increase as more people receive the vaccine.
- **E (Exposed); Figure 11** :
  No Controls: The curve in shows the number of individuals who have been exposed to the disease (infected but not yet infectious) over time without any intervention.
  With Controls: With controls in place, this curve typically shows a lower number of exposed individuals

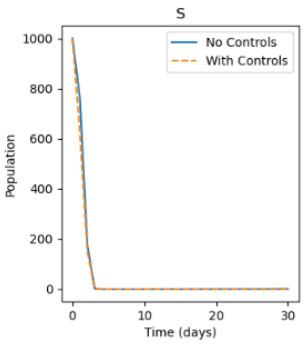

FIGURE 9. Susceptibles.

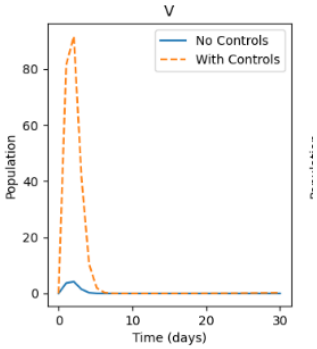

FIGURE 10. Vaccinated.

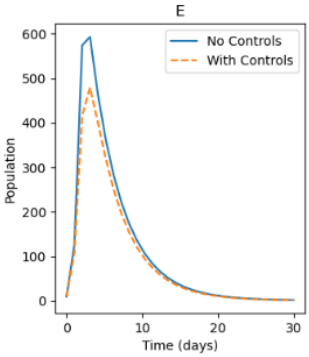

FIGURE 11. Exposed.

due to the reduced transmission rate.

- **A (Asymptomatic); Figure 12**:
  No Controls: This curve shows the number of individuals who are infected but do not show symptoms (asymptomatic carriers) over time without any intervention.
  With Controls: The curve in represents the number of asymptomatic carriers when control measures are applied. Effective controls should reduce the number of new infections and thus the number of asymptomatic carriers.
- **I (Infected);Figure 13**:
  No Controls: This curve shows the number of symptomatic infected individuals over time without any intervention.
  With Controls: This curve shows the number of symptomatic infected individuals when control measures are applied. Effective controls should result in a lower peak and fewer overall symptomatic cases.
- **J (Isolated); Figure 14**:
  No Controls: This curve shows the number of infected individuals who have been isolated (e.g., in quarantine or hospital) over time without any intervention.
  With Controls: With isolation and other control measures in place, this curve should ideally show a more controlled and possibly reduced number of isolated individuals, depending on the effectiveness of the intervention.
- **R (Recovered); Figure 15**:
  No Controls: This curve shows the number of individuals who have recovered from the disease over time without any intervention.
  With Controls: This curve shows the number of recovered individuals when control measures are applied. While controls might delay the number of new infections, eventually leading to fewer recoveries initially, it should ultimately lead to a higher number of recoveries by preventing deaths and severe cases.

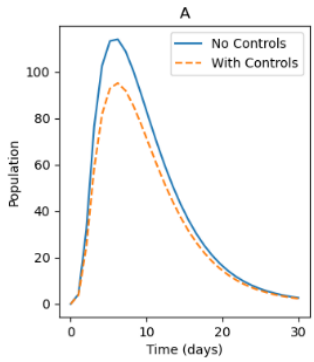

FIGURE 12. Asymptomatic.

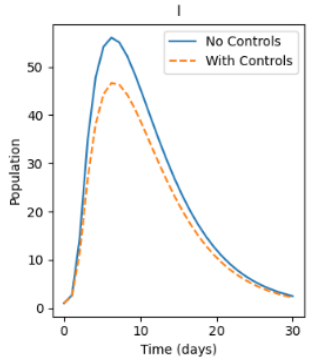

FIGURE 13. Symptomatic.

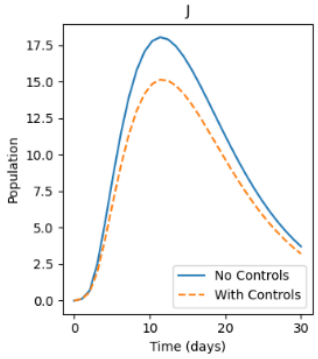

FIGURE 14. Isolated.

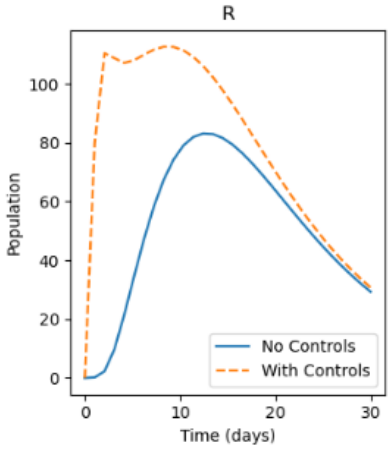

FIGURE 15. Recovered.

The curves with controls demonstrate how interventions can influence the spread and impact of the disease across different compartments of the population, typically aiming to reduce the number of susceptible, exposed, asymptomatic, symptomatic, and isolated individuals while increasing the number of vaccinated and recovered individuals.

7. Conclusion

Various mathematical models exist to forecast the number of COVID-19 infections, with the COVID-19 infection reproduction rate (R0) being a critical factor influencing the pandemic's scale and progression globally. These models serve as valuable tools for studying disease transmission dynamics and the effectiveness of social and public health interventions in managing acute infections like COVID-19.

In our study, we employed an extension of the classic SIR model developed by Kermack and McKendrick, which incorporates factors such as social distancing, imperfect vaccination, and isolation. This model enables us to analyze the impact of social distancing on disease spread and assess the effectiveness of public health interventions in controlling the pandemic.

Through theoretical analysis, we derived both the effective and basic reproduction numbers of the model. While both the disease-free and endemic equilibriums are locally stable, they are globally unstable, indicating that the disease cannot be completely eradicated if the reproduction number is below unity.

Furthermore, even with high vaccine efficacy and a large portion of the population vaccinated, complete eradication of the disease is not achieved. This highlights the need for additional measures to reduce the basic reproduction number below unity. The numerical simulation of the optimal control set in the epidemiological model illustrates how interventions such as vaccination, social distancing, and isolation can influence the spread and impact of a disease within a population. The curves representing different compartments show the evolution over time of susceptible, vaccinated, exposed, asymptomatic, symptomatic, isolated, and recovered individuals. With controls in place, the number of susceptible individuals decreases at a slower rate, the number of vaccinated individuals increases, the number of exposed individuals decreases, the number of asymptomatic and symptomatic cases is reduced, and the number of isolated individuals is more controlled. Ultimately, the goal of these interventions is to reduce the overall spread of the disease and increase the number of recovered individuals by preventing severe cases and deaths.

References

[1] F. B. Agusto, *Optimal isolation control strategies and cost-effectiveness analysis of a two-strain avian influenza model*, Biosystems, *113*(3) (2013), 155–164.

[2] A. Ayalew, Y. Molla, T. Tilahun, and T. Tesfa, *Mathematical Model and Analysis on the Impacts of Vaccination and Treatment in the Control of the COVID-19 Pandemic with Optimal Control*, Journal of Applied Mathematics, *2023* (2023).

[3] Y. Bai, L. Yao, T. Wei, F. Tian, D. Y. Jin, L. Chen, and M. Wang, *Presumed asymptomatic carrier transmission of COVID-19*, JAMA, *323*(14) (2020), 1406-1407.

[4] A. Babaei, H. Jafari, S. Banihashemi, and M. Ahmadi, *Mathematical analysis of a stochastic model for the spread of Coronavirus*, Chaos, Solitons & Fractals, *145* (2021), 110788.

[5] G. Birkhoff and G. C. Rota, *Ordinary Differential Equations*, Blaisdell Pub. Co., Waltham, Mass, (1969).

[6] S. Biswas, A. Subramanian, I. M. ELMojtaba, J. Chattopadhyay, and R. R. Sarkar, *Optimal combinations of control strategies and cost-effective analysis for visceral leishmaniasis disease transmission*, PLoS One, *12*(2) (2017), e0172465.

[7] S. P. Brand, R. Aziza, I. K. Kombe, C. N. Agoti, J. Hilton, K. S. Rock, and E. W. Barasa, *Forecasting the scale of the COVID-19 epidemic in Kenya*, MedRxiv, *2020*(04) (2020).

[8] K. M. Bubar, K. Reinholt, S. M. Kissler, M. Lipsitch, S. Cobey, Y. H. Grad, and D. B. Larremore, *Model-informed COVID-19 vaccine prioritization strategies by age and serostatus*, Science, *391*(6352) (2021), 916-921.

[9] B. Buonomo, D. Lacitignola, and C. Vargas-De-León, *Qualitative analysis and optimal control of an epidemic model with vaccination and treatment*, Mathematics and Computers in Simulation, *100* (2014), 88-102.

[10] C. Connelly, *Epidemiology Through the Lens of Differential Equations*, (2023).

[11] K. Dehingia, A. A. Mohsen, S. A. Alharbi, R. D. Alsemiry, and S. Rezapour, *Dynamical behavior of a fractional order model for within-host SARS-CoV-2*, Mathematics, *10*(13) (2022), 2344.

[12] C. T. Deressa, Y. O. Mussa, and G. F. Duressa, *Optimal control and sensitivity analysis for transmission dynamics of Coronavirus*, Results in Physics, *19* (2020), 103942.

[13] M. L. Diagne, H. Rwezaura, S. Y. Tchoumi, and J. M. Tchuenche, *A mathematical model of COVID-19 with vaccination and treatment*, Computational and Mathematical Methods in Medicine, *2021* (2021).

[14] O. Diekmann, J. A. P. Heesterbeek, and J. A. J. Metz, *On the definition and the computation of the basic reproduction ratio R0 in models for infectious diseases in heterogeneous populations*, Journal of Mathematical Biology, *28* (1990), 395-392.

[15] K. Dietz, *The estimation of the basic reproduction number for infectious diseases*, Statistical Methods in Medical Research, *2* (1993), 23–41.

[16] K. D. Elgert, *Immunology: understanding the immune system*, John Wiley & Sons, (2009).

[17] L. X. Feng, S. L. Jing, S. K. Hu, D. F. Wang, and H. F. Huo, *Modelling the effects of media coverage and quarantine on the COVID-19 infections in the UK*, Math. Biosci. Eng., *17*(4) (2020), 3918-3939.

[18] M. Fudolig and R. Howard, *The local stability of a modified multi-strain SIR model for emerging viral strains*, PLoS One, *15*(12) (2020), e0243408.

[19] Y. Gu, S. Ullah, M. A. Khan, M. Y. Alshahrani, M. Abohassan, and M. B. Riaz, *Mathematical modeling and stability analysis of COVID-19 with quarantine and isolation*, Results in Physics, *34* (2022), 105284.

[20] S. D. Gupta, R. Jain, and S. Bhatnagar, *COVID-19 pandemic in Rajasthan: Mathematical modelling and social distancing*, Journal of Health Management, *22*(2) (2020), 129-139.

[21] E. Hansen and T. Day, *Optimal control of epidemics with limited resources*, Journal of Mathematical Biology, *62* (2011), 423-451.

[22] D. La Torre, D. Liuzzi, T. Malik, O. Sharomi, and R. Zaki, *Dynamics and optimal control for a spatially-structured environmental-economic model*, Electronic Journal of Differential Equations, *2015*, 1-15.

[23] S. Lenhart and J. T. Workman, *Optimal control applied to biological models*, Chapman and Hall/CRC, 2007.

[24] Q. Li, X. Guan, P. Wu, X. Wang, L. Zhou, Y. Tong, ..., and Z. Feng, *Early transmission dynamics in Wuhan, China, of novel coronavirus–infected pneumonia*, New England Journal of Medicine, *392*(13) (2020), 1199-1207.

[25] E. T. Lofgren, M. E. Halloran, C. M. Rivers, J. M. Drake, T. C. Porco, B. Lewis, ..., and S. Eubank, *Mathematical models: A key tool for outbreak response*, Proceedings of the National Academy of Sciences, *111*(51) (2014), 18095-18096.

[26] S. Mwalili, M. Kimathi, V. Ojiambo, D. Gathungu, and R. Mbogo, *SEIR model for COVID-19 dynamics incorporating the environment and social distancing*, BMC Research Notes, *13*(1) (2020), 1-5.

[27] H. J. Namawejje, L. S. Luboobi, D. Kuznetsov, and E. Wobudeya, *Modeling optimal control of rotavirus disease with different control strategies*, Journal of Mathematical and Computational Science, *4*(5) (2014), 892.

[28] E. G. Nepomuceno, M. L. Peixoto, M. J. Lacerda, A. S. Campanharo, R. H. Takahashi, and L. A. Aguirre, *Application of optimal control of infectious diseases in a model-free scenario*, SN Computer Science, *2*(5) (2021), 405.

[29] G. Oliveira, *Refined compartmental models, asymptomatic carriers and COVID-19*, arXiv preprint, *arXiv:2004.14780*, (2020).

[30] B. Pantha, F. B. Agusto, and I. M. Elmojtaba, *Optimal control applied to a visceral leishmaniasis model*, (2020).

[31] C. A. Pearson, F. Bozzani, S. R. Procter, N. G. Davies, M. Huda, H. T. Jensen, and R. M. Eggo, *Health impact and cost-effectiveness of COVID-19 vaccination in Sindh Province Pakistan*, medRxiv, (2021).

[32] Z. H. Shen, Y. M. Chu, M. A. Khan, S. Muhammad, O. A. Al-Hartomy, and M. Higazy, *Mathematical modeling and optimal control of the COVID-19 dynamics*, Results in Physics, *31* (2021), 105028.

[33] B. Tang, X. Wang, Q. Li, N. L. Bragazzi, S. Tang, Y. Xiao, and J. Wu, *Estimation of the transmission risk of the 2019-nCoV and its implication for public health interventions*, Journal of Clinical Medicine, *9*(2) (2020), 462.

[34] P. Van Den Driessche and J. Watmough, *Further notes on the basic reproduction number*, Mathematical Epidemiology, (2008), 159-178.

[35] H. M. Wanjala, M. O. Okongo, and J. O. Ochwach, *Impact of Media Awareness and Use of Face-Masks on Infectious Respiratory Disease*, Pan-American Journal of Mathematics, *2* (2023), 15.

[36] H. M. Wanjala, M. Okongo, and J. Ochwach, *Mathematical Model of the Impact of Home-Based Care on Contagious Respiratory Illness Under Optimal Conditions*, Jambura Journal of Biomathematics (JJBM), *5*(2) (2024), 83-94.

[37] I. M. Wangari, S. Sewe, G. Kimathi, M. Wainaina, V. Kitetu, and W. Kaluki, *Mathematical modelling of COVID-19 transmission in Kenya: a model with reinfection transmission mechanism*, Computational and Mathematical Methods in Medicine, *2021* (2021).

[38] L. Yao, T. Wei, F. Tian, D. Y. Jin, L. Chen, and M. Wang, *Presumed asymptomatic carrier transmission of COVID-19*, JAMA, *323*(14) (2020), 1406-1407.

[39] X. M. Zhang and Q. L. Han, *New Lyapunov-Krasovskii functionals for global asymptotic stability of delayed neural networks*, IEEE Transactions on Neural Networks, *20*(3) (2009), 533-539.